We are IntechOpen, the world's leading publisher of Open Access books Built by scientists, for scientists

6,900
Open access books available

186,000
International authors and editors

200M
Downloads

Our authors are among the

154
Countries delivered to

TOP 1%
most cited scientists

12.2%
Contributors from top 500 universities

CLARIVATE ANALYTICS
BOOK CITATION INDEX
INDEXED

WEB OF SCIENCE™

Selection of our books indexed in the Book Citation Index
in Web of Science™ Core Collection (BKCI)

Interested in publishing with us?
Contact book.department@intechopen.com

Numbers displayed above are based on latest data collected.
For more information visit www.intechopen.com

Undulators for Short Pulse X-Ray Self-Amplified Spontaneous Emission-Free Electron Lasers

K. Zhukovsky

Additional information is available at the end of the chapter

Abstract

We review the synchrotron type radiation sources with focus on undulator and free-electron laser (FEL) schemes, aimed on working in X-ray range and ultra-short time interval. Main FEL schemes, useful for generation of high frequency radiation, extending to X-rays, are presented. High harmonic generation is explored. The advantages and disadvantages of single pass and of multipass designs are discussed. The viable ways to reduce the duration of the pulse, with the goal to generate femtosecond pulses, are indicated. Future developments of X-ray FELs (X-FELs) and the ways to improve the quality of the FEL radiation in this context are discussed.

Keywords: undulator radiation, harmonics generation and broadening, homogeneous and inhomogeneous losses, free-electron laser

1. Introduction

Synchrotron radiation (SR) and undulator radiation (UR) have been attracting researcher's attention for more than half a century. The reasons for that varied with time passing as the challenges for the scientists evolved and the technical progress stepped forward. UR was predicted [1] and then discovered [2] in the middle of the twentieth century. During the following 70 years, the study of the radiation, emitted by ultra-relativistic electrons, was performed, and the SR theory was refined; extensive theoretical studies of the electron motion in periodic magnetic fields of various configurations have been performed [3–7]. Now UR is

again in focus due to the request for coherent X-ray sources [8], while free-electron lasers (FELs) extend to X-range [9]. Both, SR and UR are due to the radiation of relativistic electrons, executing curved trajectories [10]. The difference between them is in the length on which the radiation is formed: short part of the circle for UR and the full length of the undulator for the UR. This determines the fundamental difference in the quality of the radiation obtained from these two sources: short pulses with very broad spectrum for the SR and relatively long-lasting radiation bursts with narrow spectrum for the UR. Nowadays, the research frontier is represented by studies of ultra short attosecond time intervals and Röntgen range [11, 12]. To achieve these characteristics, the devices require extremely high quality and intense magnetic fields, long undulators with many periods. To obtain high frequency radiation, sometimes undulator periodic structures with double or even triple period are used [13–18], facilitating control over high harmonics and regulating their emission [6, 19]. Maintaining best quality UR line is important. Nowadays, electron accelerators provide ultra fast and high coherent electron beams and intense emission even in Röntgen range. Modern undulators allow for the harmonic emission regulation [19], which can be achieved by superimposing different periodic magnetic fields in many period undulators. It should be noted that in long undulators the distortions of the magnetic field and of unavoidable inhomogeneities of periodic magnetic field have very strong effect on the operation of the devices. High gain in undulators is essential in FEL with self-amplified spontaneous emission (SASE), with high-gain harmonic generation (HGHG), and in other modern schemes. The quality of the electron beams, fed into the undulators, is extremely important for such new FELs [20], in particular at high frequencies. The requirements for the periodicity of the field are particularly rigid in long undulators [21]. Deviation from the ideal oscillatory trajectories of electrons results in degradation of the beam quality and of the FEL output in terms of power, brightness FEL gain. Therefore, the emitted UR can be exploited for diagnosing the quality of the undulator itself.

The radiation spectrum lines from undulators inevitably broaden due to a number of reasons, first of all due to the electron beam energy spread and the beam divergency, as well as due to inhomogeneity of the periodic magnetic field in undulators. They may have internal or external origin [22–26], but their presence is eminent also due to the fact that the ideal $\vec{H} = H_0 sin(2\pi z / \lambda)$ periodic magnetic field simply does not satisfy Maxwell equations. The electron energy spread is the most common detrimental factor; some researchers even concluded that the spectral properties of higher UR harmonics should be limited only by the electron beam properties and not by the undulators [24]. The role of the divergence was underlined, for example, in Refs. [22, 27]. At the same time the constant magnetic field shifts the resonance frequencies and causes loss of intensity [28–31].

The demand for radiation with specific properties and high requirement to the UR and undulator quality stimulated analytical study of their spectral properties [32–39]. There appear generalized Bessel and Airy functions naturally, as well as in other mathematical problems of radiation, emitted by charges, executing complicated oscillating trajectories. The mathematical apparatus of inverse differential operators and orthogonal polynomials was developed for treating broad spectrum of physical problems, which include radiation and propagation of

electron beams [40–45]. The contributions of all sources of broadening in various undulator schemes were analyzed by means of precise analytical treatment of the UR, employing extended forms of special functions of Airy and Bessel types [34–37, 39, 42]. In these works, the role of the various broadening terms, accounting for the real size and the emittance of the electron beam, for the energy spread and for the constant field component, was explored. It was shown that the undulator length has strong detrimental effect on the spontaneous harmonic emission; partial compensation of the beam divergences by constant magnets was also demonstrated.

2. Synchrotron radiation, undulator radiation, and free-electron lasers

Charged particle radiates energy in the form of electromagnetic radiation when it accelerates. Following relativistic Lorentz transforms $\tan\theta = \frac{\sin\theta'}{\gamma(\beta + \cos\theta')}$, it is easy to conclude that the radiation emission of the relativistic electron is focused in the narrow angle $\theta \approx \frac{1}{\gamma}$ (see, for example, [46]). While the charge is moving on a circular orbit of radius R, it emits SR in a narrow cone of emission, which illuminates the receiver for a very short period of time, while passing from the point A to the point B. Lorentz transforms is applied to the period of time in the reference frames, related to the electron and to the observer and yield the time of the SR pulse $\Delta t = \frac{m}{2eB\gamma^2} = \frac{R}{2c\gamma^3}$, where $R \cong \frac{\gamma mc}{eB}$. For the UR, it is not so, since it is gathered all along the undulator and the characteristic length then equals that of the undulator, by far exceeding the arc, from which the SR, reaching the user, is gathered. Denoting the unit vector $\vec{n} = \vec{R}/R$ and $\vec{n} \cong (\psi\cos\phi,\ \psi\sin\phi,\ 1-\psi^2/2)$, it is easy to obtain the wavelength of the radiation, emitted off the axis in the angle θ

$$\lambda_n = \frac{\lambda_u}{2n\gamma^2}\left(1 + \gamma^2\left\langle\theta^2\right\rangle + \gamma^2\psi^2\right) \tag{1}$$

from the simple condition of positive interference of the wavelengths, emitted on each magnetic poles of the undulator. Since the SR from a relativistic charge is emitted in a narrow cone, which includes the undulator axis all the time, the electron drifts in the undulator at relativistic speed, if the electrons transversal oscillations are small. At the exit of the undulator the intense radiation appears (see **Figure 1**).

The spectral range of SR and UR extends up to Röntgen band. However, due to the fact that the SR is perceived as a very short pulse, its spectral range is very broad, starting from the synchrotron frequency $\omega_0 = v/R$, while the UR has few harmonics and in some cases, such as that of a spiral undulator, it can contain a single harmonic.
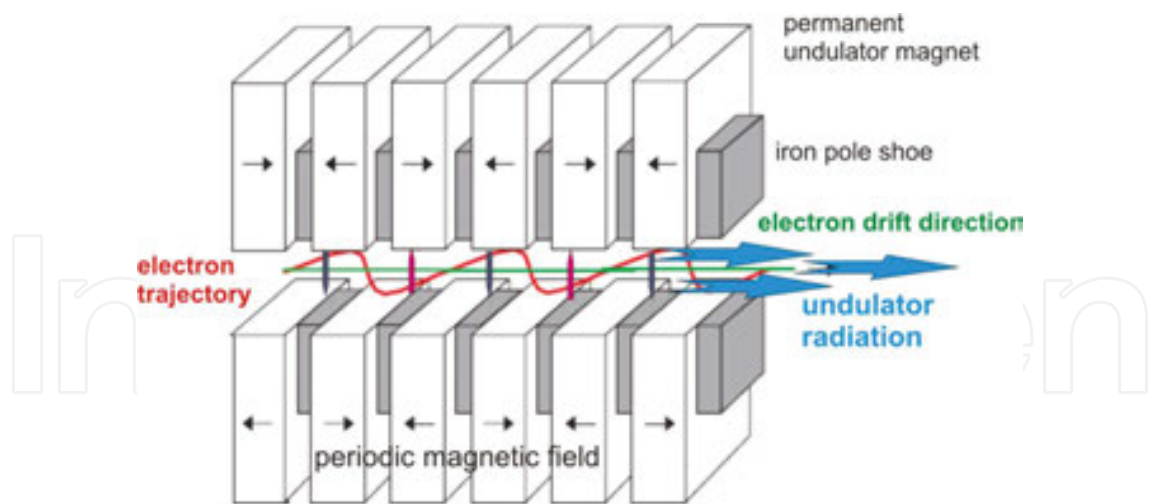
Figure 1. Schematic drawing of a planar undulator.

For spontaneous radiation, emitted by an electron, the undulator selects resonant UR wavelengths. The idea about it can be given by the simple consideration, demonstrated in **Figure 2**, where electric fields for two resonant wavelengths λ_n at the fundamental ($n = 1$; red) and at the third harmonics ($n = 3$; blue) are shown. A non-resonant electric field for the second harmonic is shown in green. The fundamental and the third harmonics are phase-matched with the electron after one undulator period as highlighted in **Figure 2**. The electron trajectory is drawn in gray. Such a phase matching of the radiation proceeds on each next undulator period. Thus, the radiation from one electron constructively interferes over many periods, and in this sense we obtain coherent radiation from one electron along the whole length of the undulator.
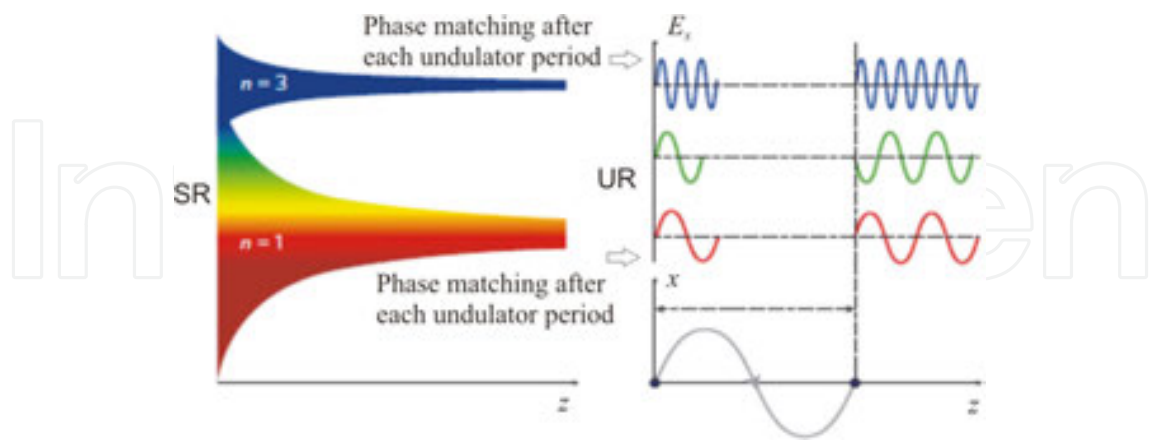

Figure 2. Undulator selects resonant frequencies for the emitted SR.

The following conditions are common in modern undulators: the electrons are ultrarelativistic, which is natural in contemporary accelerators, they have small transverse momentum, and the electric field is absent:

$$\gamma \gg 1, \beta_\perp \ll 1, H_{||} \ll H_\perp, \vec{E} = 0 \tag{2}$$

The UR from a planar undulator with N periods of λ_0 with the undulator parameter $k = \dfrac{e}{mc^2}\dfrac{H_0}{k_\lambda}$, where $k_\lambda = 2\pi/\lambda_u$, λ_u is the undulator period, $H_y = H_0 sin(k_\lambda z)$ is the sinusoidal magnetic field, has the following peak frequencies:

$$\omega_n = n\omega_R = \frac{2n\omega_0\gamma^2}{1 + \dfrac{k^2}{2} + (\gamma\psi)^2}, \quad \omega_{R0} = \frac{2\omega_0\gamma^2}{1 + k^2/2}, \quad \omega_{n0} = n\omega_{R0}, \tag{3}$$

where $\omega_0 = k_\lambda\beta_z^0 c$, $\beta_z^0 = 1 - \dfrac{1}{2\gamma^2}\left(1 + \dfrac{k^2}{2}\right)$ is the average drift speed of the electrons along the undulator axis, $k \approx H_0\lambda_0$ $[Tcm]$ and ψ is off the undulator axis angle. The shape of the UR emission line is described by the $\dfrac{sin(\nu_n/2)}{\nu_n/2} = sinc\dfrac{\nu_n}{2}$ function, dependent on the detuning parameter

$$\nu_n = 2\pi Nn\left(\frac{\omega}{\omega_n} - 1\right). \tag{4}$$

The homogeneous bandwidth, sometimes called half-width of UR spectrum line at its half-height or simply half-width, is $\dfrac{1}{2nN}$ and the half-width equals

$$\frac{\Delta\omega}{\omega_{n0}} = \frac{\omega - \omega_{n0}}{\omega_{n0}} = \frac{1}{nN}. \tag{5}$$

In real devices $\dfrac{1}{nN} \ll 1$. The emitted wavelength $\lambda_n = 2\pi/k_n$ can be expressed through the speed of the electrons in the undulator as follows:

$$\lambda_n = \frac{\lambda_1}{n} = \frac{\lambda_u}{n}\left(\frac{1 - u/c}{u/c}\right) \cong \frac{\lambda_u}{2n\gamma^2}\left(1 + \tilde{k}^2\right), \tag{6}$$

where λ_u is the undulator period, u is the electron speed

$$u = c\left(1 - \left(1 + \tilde{k}^2\right)\big/2\gamma^2\right), \tag{7}$$

The undulator parameter is k or $\tilde{k}$:

$$\tilde{k}^2 \equiv \frac{k^2}{2} = \gamma^2 \beta_\perp^2 = \gamma^2 \left\langle \theta^2 \right\rangle, \, k = eH_0 \lambda_u / 2\pi mc^2, \tag{8}$$

θ is the off-axis angle, which in essence indicates how much the electron deviates from the axis in its motion along the undulator due to transversal oscillations, caused by the periodic magnetic field. In real conditions for a weak undulator $k \sim 1$, while for wiggler or strong undulator $k \sim 10$. Thus, for a weak undulator the radiation is essentially directed all along the undulator axis, while for the wiggler, it is in much wider angle. Considering $n = 1$, i.e., the fundamental harmonic, we write $u = ck_1/(k_1 + k_u)$, $k_1 = 2\pi/\lambda_1$. Both SR and spontaneous UR are incoherent. In the full spectrum of the radiation, the components, whose wave length is longer than the bunch length, are coherent, while the radiation of the length, significantly exceeding the size of the bunch, is approximately coherent. The region of coherent radiation will enlarge as the bunch gets shorter. The difference between the radiations, emitted by various SR sources, is demonstrated in **Figure 3**. It shows how the radiation intensity and the degree of coherency of the emitted radiation varies from one device scheme to the other; N_f is the number of emitted photons, N_e is the number of the electrons in the beam, N is the number of undulator periods. For SR from a bending magnet, the intensity is roughly proportional to the number of electrons emitting photons in a bending magnet. Wiggler, or strong undulator, is essentially a number of bending magnets, where electrons deviate significantly from the axis; the character of the radiation remains that from the bending magnets, but the intensity is N times higher. The radiation is incoherent. In a weak undulator, where the electrons slightly oscillate in transversal to the axis plane, so that the cone of the emission of the radiation always includes the undulator axis, the radiation of one single electron is coherent along the undulator axis, but the radiation of the bunch of electrons is incoherent in between them. The intensity of the radiation is proportional to N^2. In free-electron laser, the electrons within a bunch emit largely coherent radiation, which transforms into a significant increase of the intensity $N_f \sim (N_e N)^2$.

New type of radiation source—X-ray free-electron laser (X-FEL)—provides a combination of sub-picosecond pulse duration of a conventional laser with the X-ray wavelength of a synchrotron radiation source. Practical research potential of short wave radiation in nature and in technology can hardly be overestimated. Indeed, wavelength about 200 nm allows study of viruses, the scale of an atomic corral is ~14 nm, and the wavelength of 1–2 nm gives the potential to resolve DNA helix width and carbon nanotubes, while shorter wavelengths could visualize the small molecules, such as water molecule, and atoms. On the other hand, studies of processes at mircoscale often require very short time resolution. Indeed, the processes of a water molecule dissociation takes as short time as 10 fs, Bohr period of valence electron is ~1 fs, shock wave propagates by 1 atom in 100 fs, and electron spin processes in the magnetic field of 1 T within 10 ps. Thus, it is of great practical importance to have a device, which produces radiation with a combination of very short wavelength and short duration. One of the most prominent devices of such a kind is a free-electron laser.
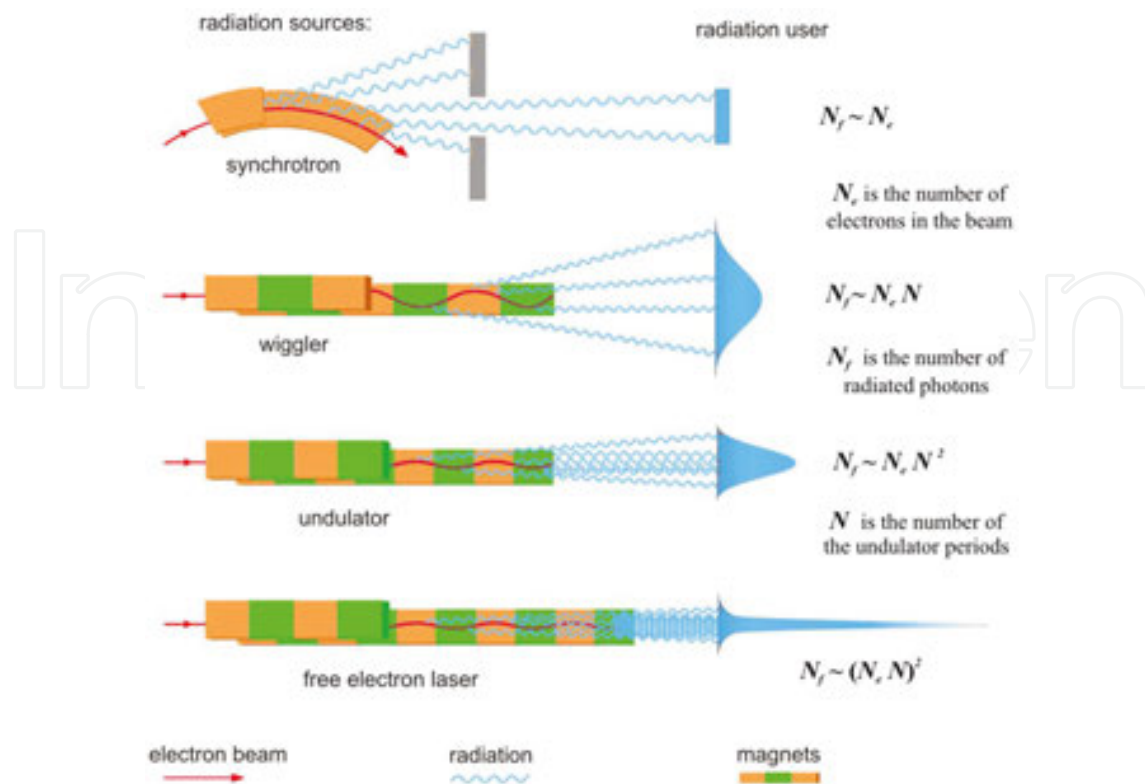
Figure 3. Different sources of SR: synchrotron, wiggler, undulator, and free-electron laser.

3. Keynotes on free-electron lasers

In 1971, Madey published a theory of the FEL [47], where he described a small gain process in a system: relativistic electron beam/undulator. In his study he hypothesized that it could generate coherent X-ray radiation. Few years later the first demonstration of FEL amplification and lasing was performed in a low-gain infrared oscillator FEL at Stanford. At approximately the same time, Colson and Hopf described classically the FEL interaction, which had god quantum description by Madey before. Since 1970s, extensive classical description of the high-gain regime of FEL operation has been developed. Since the first X-rays were discovered by Wilhelm Röntgen in Würzburg in 1895, the peak "brilliance" of X-ray sources has increased by ~16 orders of magnitude. The so-called first-generation synchrotron sources were in fact particle accelerators, designed for experiments in high-energy physics. The second-generation labs were custom-built facilities, while the third-generation sources at labs such as the European Synchrotron Radiation Facility (ESRF) feature undulators, emitting light in a very narrow cone. The fourth generation of synchrotron-radiation sources includes free-electron lasers.

To account for the processes, which occur in a free-electron laser, we need to understand the fundamental difference between the coherent and non-coherent radiation, emitted by many electrons, which pass through undulator at the same time. The power, emitted by electrons

$$P \propto \left| \sum_{j=1}^{N_e} E_j e^{i\varphi_j} \right|^2 = \sum_{j=1}^{N_e} E_j^2 + \left| \sum_{j=1, j\neq k}^{N_e} \sum_{k=1}^{N_e} E_j E_k e^{i(\varphi_j + \varphi_k)} \right|^2, \tag{9}$$

where φ_j are the relative phases of the emitted radiation electric fields E_j in a system of big number of electrons $N \gg 1$, includes two terms. For a system with uncorrelated phases, the terms in the second double sum, which is of the order of $\sim N^2$, tend to destructively interfere. This happens in incoherent spontaneous UR sources. Total power emitted then approximately equals to the sum of the powers from the N independent scattering electrons, which originates from the first term in Eq. (9). For correlated phases of the electric fields, we have $\varphi_j \approx \varphi_k$ for all the electrons and then the coherent second term $\sim N^2$ contributes. For it to happen, the electron sources must be periodically bunched at the resonant radiation wavelength. **Figure 4** demonstrates how incoherent radiation from a bunch of electrons in an undulator becomes coherent toward the undulator's end. Indeed, at the beginning, the electrons in the bunch enter the undulator with initially random phases, which ensures that mostly incoherent radiation is emitted at the resonant radiation wavelength. Because of the electrons interact collectively with the radiation they emit, small coherent fluctuations in the radiation field grow along the undulator length and simultaneously begin to bunch the electrons at the resonant wavelength. This collective process continues until the electrons are strongly bunched toward the end of the undulator, where the process saturates and the electrons begin to de-bunch.
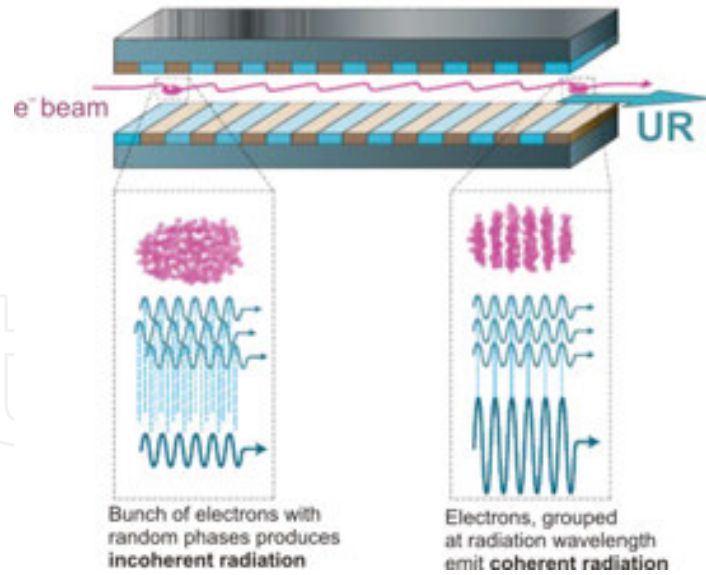

Figure 4. From incoherent to coherent emission along the undulator length.

Behind this phenomenon stands a simple physical mechanism, which is based on the fact that the speed of electrons, while being close to that of the radiation, is still smaller, and, therefore, the electrons appear behind its radiation, propagating in the undulator. It can be best illustrated in **Figure 5**.
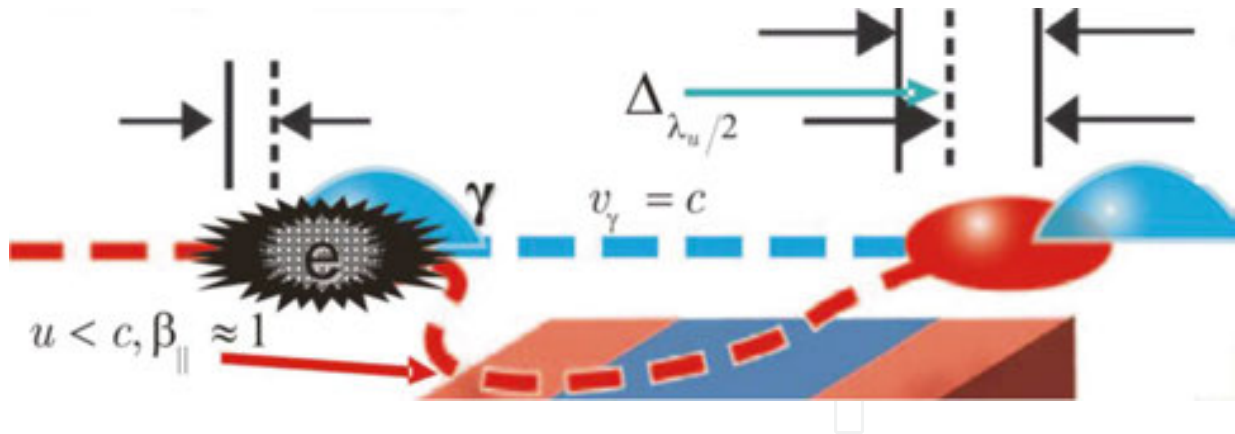
Figure 5. Slippage of the radiation and the electron bunch in FEL.

Indeed, the photons move at the speed of light $v_\gamma = c$, while the electrons move at the speed $u < c$, $\beta_{||} \approx 1$, i.e., slower than photons. Therefore a full slip between the electron bunch and the photon pulse accumulates along the length of the undulator and reads as follows:

$$\Delta = (1 - \beta_{||}) N \lambda_u \cong N\lambda, \tag{10}$$

where λ is the emitted wavelength $\lambda = \dfrac{\lambda_u}{2\gamma^2}\left(1 + \dfrac{k^2}{2}\right)$ and the parallel component of the β is $\beta_{||} \cong 1 - \dfrac{1}{2\gamma^2}\left(1 + \dfrac{k^2}{2}\right)$. Thus the slip on the whole undulator length is N times the emitted wavelength. Respectively, the slip on a distance, equal half an undulator period equals half of the emitted wavelength:

$$\Delta_{\lambda_u/2} = N\lambda/(2N) = \lambda/2. \tag{11}$$

In other words, as the radiation wave travels over a distance $\lambda/2$ in a time $\lambda/(2c)$, the electron travels over a smaller distance $u\lambda/(2c)$, and on one undulator period the electrons slip, respectively, to the photons by one emitted wavelength. The whole photon packet, having a higher velocity that the electrons, slips over the electron packet and the wave emitted by the electrons on a certain undulator period comes in phase with the wave, emitted on the next undulator period. To illustrate the formation of microbunches, which lead to coherent radiation of the electrons within a bunch, we present the following explanation in **Figure 6** (see [48]).

Suppose we have the magnetic field B_w of the already existing electromagnetic wave. Then its interaction with the electron transverse velocity v_t creates Lorentz force F_{bunch}, which we denote as f for brevity (see **Figure 6**). This force pushes the electron toward a wave node as seen in **Figure 6**. After the electron travels over one-half undulator period, its transverse velocity becomes reversed. In the meantime the electromagnetic wave travels ahead of the electron by one-half wavelength as follows from (10) and (11). Its field B_w is now also reversed, so that the

Lorentz force keeps its direction and the microbunching continues. For the charge, which is ahead with respect to the microbunch, which is in the wave node (see **Figure 6**), the Lorentz force F_{bunch} or f pushes the charge back to the node, thus grouping electrons in a bunch at the wave node. So it proceeds on other periods, because while the electrons move through a full oscillation period λ_u, the electromagnetic wave propagates by λ_u plus one wavelength λ. Consequently, the transverse movement of each electron has a constant phase with respect to the electromagnetic field.
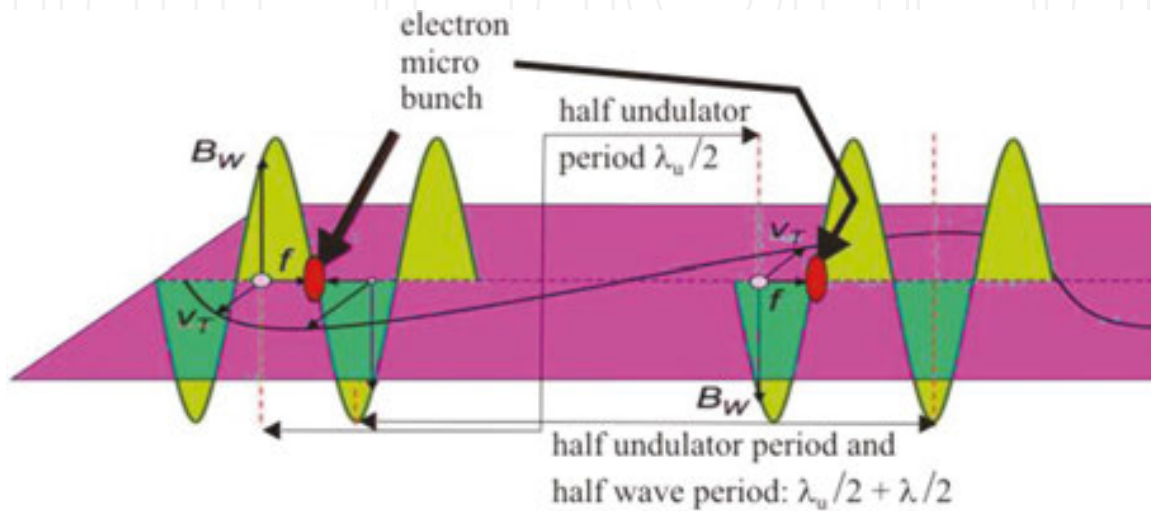

Figure 6. Interaction of the radiation with the electrons and formation of microbunches.

4. Correlated amplification in FEL

Amplification in FEL occurs because of the energy is transferred from the electrons to the previously emitted waves. This effect is due to the negative work of the force, produced by the transverse electric field of the wave, since the magnetic field of the wave does not work. The time rate of the energy transfer for a single electron is proportional to the product $E_W v_t$, where E_W is the electric field of the radiation wave and v_t is the electron transverse velocity. Then $E_W \propto I^{1/2}$, where I is the wave intensity and $dI/dt \propto I^{1/2} v_t$. Note that uncorrelated combination of the effects of individual electrons would not lead to an exponential increase of the intensity with the distance (or time), but to a quadratic law: $I(z) \propto z^2$. Transverse velocity and the field B produce longitudinal Lorentz force $F_{bunch} = v_t B_W$, which pushes the electrons and forms microbunches. This force is proportional to the transverse electron velocity, and it is also orthogonal to the wave field B of the strength B_W. Since $B_W \propto I^{1/2}$, the microbunching force is also proportional to $I^{1/2}$: $B_{bunch} \propto I^{1/2}$. We now assume that this force enhances the correlated emission by a factor, proportional to the microbunching force. Multiplied by the energy

transfer rate for each electron, this factor gives $dI/dt = AI$, A = constant. Proceeding on the supposition that $A = u/L_G$, where L_G is the gain length, we obtain the exponential growth:

$$I = I_0 \exp\left(\frac{ut}{L_G}\right) = I_0 \exp\left(\frac{z}{L_G}\right). \tag{12}$$

The exponential gain only occurs after bunching is established. This process continues until the saturation is reached. Provided at the beginning, the initial position of the electron, respectively, the existing wave, is favorable for the energy transfer from the electron to the wave and the direction of the electron transverse velocity, respectively, to the wave electric field E result in negative work, the electron energy is successfully transferred to the wave. This results in the decrease in the electron energy and of the longitudinal speed of the electron u, which becomes $u - \Delta u$. This decrease in longitudinal speed in its turn changes the above conditions, making them less favorable for the energy transfer from the electron to wave. At a certain point, as this process continues and the electron speed reduction Δu becomes more and more significant, the electrons can give no more energy to the wave and the wave starts giving its energy to the electrons of the beam. It increases the electron speed u and restores the favorable for the energy transfer from the electrons to the wave conditions. Thus, in this regime the exponential wave energy growth is over and instead the energy oscillates between the wave and the electrons.

To find the amplification value, we must evaluate v_t and the degree of bunching. The transverse speed of the electron reads as follows:

$$v_t = \left(\frac{euH_0}{\gamma m_0}\right)\left(\frac{\lambda_u}{2\pi u}\right)\cos\frac{2\pi ut}{\lambda_u}. \tag{13}$$

The energy transfer rate by a single electron to preexisting wave is proportional to $I^{1/2}H_0\lambda_u/\gamma$; the field B_W of the electromagnetic wave is proportional to the square root of the wave intensity $B_W \propto I_0^{1/2}\exp\left(ut/2L_G\right)$. Then the bunching force, which is the longitudinal force, can be written as follows:

$$F_{\text{bunch}} = \text{const} \times \left(\frac{H_0\lambda_u}{\gamma}\right)I_0^{1/2}\exp\left(\frac{ut}{2L_G}\right), \tag{14}$$

which, in turn, yields the following equation of motion for longitudinal mass $\gamma^3 m$:

$$\gamma^3 m \frac{d^2 \Delta x}{dt^2} = F_{\text{bunch}} = \text{const} \times \left(\frac{H_0 \lambda_u}{\gamma} \right) I_0^{1/2} \exp \left(\frac{ut}{2L_G} \right). \tag{15}$$

The bunching force F_{bunch} induces a small longitudinal electron displacement Δx:

$$\Delta x = \text{const} \times \frac{1}{\gamma^3} \frac{H_0 \lambda_u}{\gamma} L_G^2 I_0^{1/2} \exp \left(\frac{ut}{2L_G} \right) = \frac{H_0 \lambda_u L_G^2}{\gamma^4} I^{1/2}. \tag{16}$$

As discussed above, the electrons are concentrated in narrow slabs, separated from each other by a distance of the wavelength λ. The degree of microbunching, corresponding to the fraction of electrons that emit in a correlated way, can be assumed to be proportional to $(\Delta x/\lambda)$. The corresponding number of electrons is proportional to $N_e(\Delta x/\lambda)$. Their contribution to the wave intensity reads as follows:

$$j \frac{\Delta x}{\lambda} \propto j \frac{I^{1/2} H_0 \lambda_u L_G^2 / \gamma^4}{\lambda_u / \gamma^2} = j I^{1/2} H_0 L_G^2 / \gamma^2, \quad j \equiv \frac{i}{\Sigma} = \frac{\text{current}}{\text{cross-section}}. \tag{17}$$

Microbunching effects correspond to a factor, proportional to the longitudinal microbunching force F_{bunch} and, therefore, proportional to $\sim I^{1/2}$, where I is the electromagnetic wave intensity. Multiplying this factor by the energy transfer rate for electrons, we obtain the total transfer rate as follows:

$$\frac{dI}{dt} = \text{const} \times j \frac{H_0 L_G^2}{\gamma^2} I^{1/2} \left(I^{1/2} \frac{H_0 \lambda_u}{\gamma} \right) = \text{const} \times j \frac{H_0^2 \lambda_u L_G^2}{\gamma^3} I. \tag{18}$$

The solution of this equation reads $I = I_0 \exp(z/L_G)$ and for ultrarelativistic electrons $u/L_G \cong c/L_G \propto j H_0^2 \lambda_u L_G^2 / \gamma^3$. Thus we obtain the FEL gain length

$$L_G = \text{const} \times j^{-1/3} H_0^{-2/3} \lambda_u^{-1/3} \gamma. \tag{19}$$

Gain length is related to the Pierce parameter as follows:

$$\rho = \frac{\lambda_u}{4\pi \sqrt{3} L_G} \propto j^{1/3} H_0^{2/3} \lambda_u^{4/3} \gamma^{-1} \tag{20}$$

which can be also written as $\rho = \frac{1}{2\gamma}\left(\frac{I_e}{I_A}\left(\frac{\lambda_u \tilde{k} f_B}{2\pi\sigma_r}\right)^2\right)^{1/3}$, where $I_A \cong 17$ kA is the Alfven current, I_e is the electron beam current, σ_r is the beam radius, $f_B(J_n)$ is the bunching coefficient, and J_n are the Bessel functions. The arguments and the varieties of the Bessel functions, in charge of the description of the harmonics of the UR, will be explored in what follows.

5. Cavity-based FELs

There are essentially two main types of design for FEL: cavity-based FELs and single-pass FELs. Cavity-based FELs exploit many passes of the UR in the undulator and use mirrors. Relativistic electron beam passes through periodic magnetic field of an undulator and the mirrors feed spontaneous emission back onto the beam. Consequently, the spontaneous emission is enhanced by the stimulated emission.
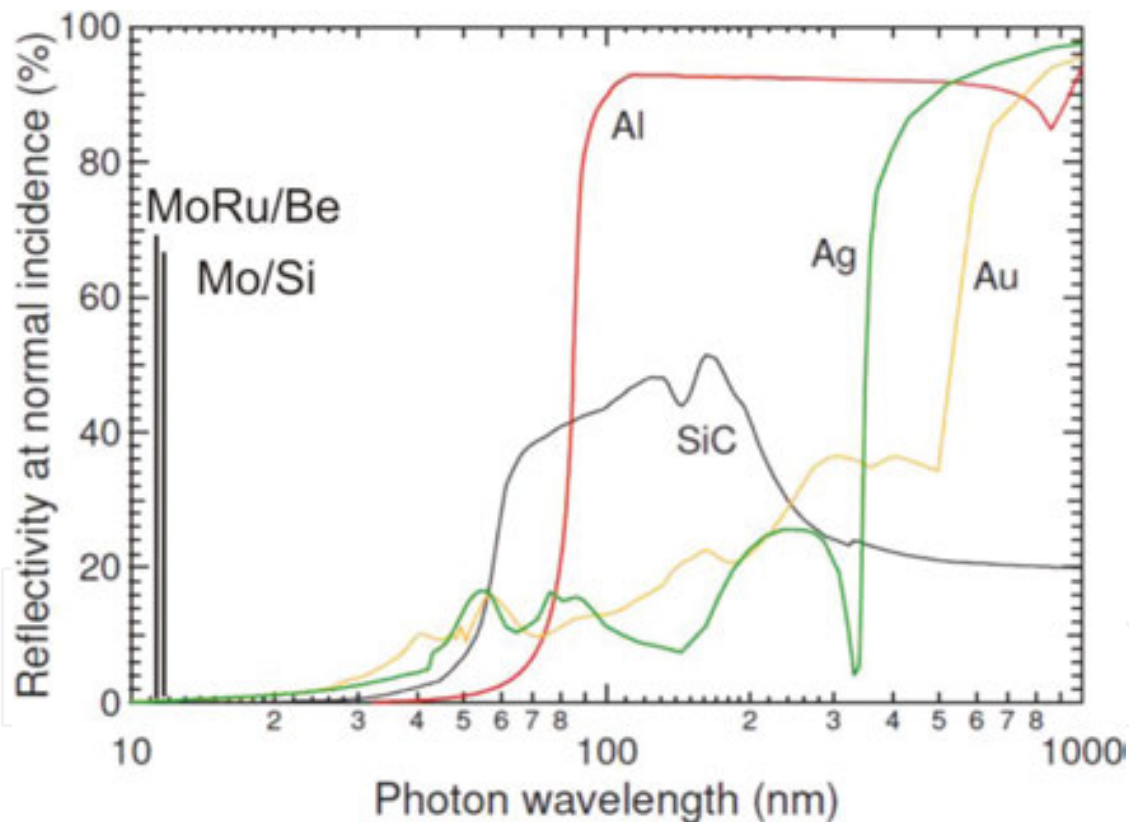

Figure 7. FEL mirror limitations.

Mirror design imposes limitations on the wavelength due to the mirror material. Common mirror materials limit the wavelength to IR-UV (see **Figure 7**). Recent improvements in materials and technology result in new multilayer X-ray reflective mirrors, which have the efficiency up to 70%, such as MoRu/Be mirrors have 69.3% reflectivity maximums at 11.43 nm, Mo/Si mirrors have 67.2% reflectivity peak at 13.51 nm.
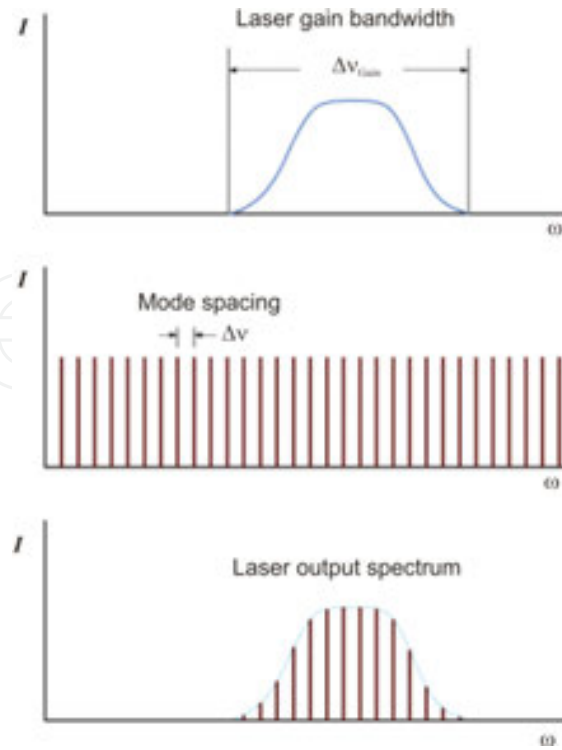
Figure 8. Longitudinal mode structure in mirror-based FEL design.

The mirror design has significant advantage: mirrors naturally select longitudinal modes, which are determined by the integer number of half-periods of the wavelength in between them. The longitudinal modes in optical cavity are equally spaced in frequency and time (see the middle plot in **Figure 8**):

$$\Delta v = \frac{c}{2L}, \Delta \tau = \frac{1}{\Delta v}. \tag{21}$$

The interval between them depends on the cavity length L (see the middle plot in **Figure 8**).

Taking into account the laser gain bandwidth

$$\Delta v_{\text{Gain}} \approx \frac{1}{\tau_{\text{Pulse}}} = \frac{c}{2\Delta} \tag{22}$$

where $\Delta = N\lambda$ (see (10), see the top plot in **Figure 8**) and, imposing it on the longitudinal picture of the middle plot in **Figure 8**, we obtain the laser spectrum as shown in the bottom plot of **Figure 8**. Inside the gain bandwidth, the longitudinal modes of the laser will periodically and constructively interfere with each other when in phase, producing an intense burst of light. These light bursts are separated by the period of time $\tau = 2L/c$, necessary for the light to make

exactly one round trip of the laser cavity; the comb of equally spaced modes in the output spectrum with spacing

$$\Delta \nu_{\mathrm{RoundTrip}} = \Delta \nu = \frac{1}{\tau_{\mathrm{RoundTrip}}}, \text{ where } \tau_{\mathrm{RoundTrip}} = \frac{2L}{c} \tag{23}$$

and L is the cavity size. In other words, only phase-matched wavelengths will constructively interfere and form the modes of the radiation field to create a comb of equally spaced modes in the output frequency spectrum. Such a laser is said to be mode-locked or phase-locked. Mode locking modifies the temporal envelope of the output field from a continuous wave to a series of short, periodically spaced pulses. The homogeneous gain bandwidth of a FEL is determined by the slippage length $\Delta = N\lambda$ (10). This last plays central role in FEL physics. Indeed, it is easy to see that only finite number of longitudinal modes with positive gain N_{Gain} exist: $\Delta \nu_{\mathrm{Gain}} \approx \frac{1}{\tau_{\mathrm{Pulse}}} = \frac{c}{2\Delta}$ (see (21)–(23)), where $\Delta = N\lambda$, λ is the radiated wavelength, and N is the number of the undulator periods. Therefore the number of gained modes reads as follows:

$$N_{\mathrm{Gain}} = \frac{\Delta \nu_{\mathrm{Gain}}}{\Delta \nu_{\mathrm{RoundTrip}}} \approx \frac{L}{\Delta}, \tag{24}$$

and the duration of the pulse is evidently

$$\tau_{\mathrm{Pulse}} \approx \frac{1}{\Delta \nu_{\mathrm{Gain}}} = \frac{\tau_{\mathrm{RoundTrip}}}{N_{\mathrm{Gain}}}. \tag{25}$$

For a Gaussian-shaped pulse, we have $\tau_{\mathrm{Gaussian\,Pulse}} \cong \frac{0.44}{\Delta \nu_{\mathrm{Gain}}}$. Thus, a laser macro pulse of, to say, microsecond duration consist of a train of short micro pulses, which are picoseconds or less in length. Such a short duration of the pulses is useful for studies of ultrashort physical and chemical processes. It is used for ultrafast spectroscopy and in femto-chemistry. The macro pulses repeat at a repetition ratio, limited by the accelerator usually at 10–100 Hz. The micro pulse repetition rate can vary from several MHz to even THz.

We omit in this work the field gain equations, which are well known and can be found elsewhere, and without derivation we just state the formulation of the Madey's theorem [47], which claims that the gain in the so-called Compton or low-gain regime is proportional to the slope of the spontaneous UR spectrum $f(\nu)$: $G(\nu) \propto \frac{\partial f(\nu)}{\partial \nu}$, $f(\nu) = sinc^2(\nu)$, and, therefore,

$$G(\nu) = -\frac{j}{2} \partial_\nu \left[\sin \frac{\nu}{2} \middle/ \frac{\nu}{2} \right]^2, \tag{26}$$

where j is the current density, v is the detuning parameter (4). **Figure 9** demonstrates the FEL gain; the homogeneous bandwidth is given by $\frac{\Delta\omega}{\omega_0} = \frac{1}{2N}$. In the presence of constant magnetic field, the line shape is described by the Airy-type function $S(v_n, \beta) \equiv \int_0^1 d\tau e^{i(v_n\tau + \beta\tau^3)}$ and the derivative modifies into $-\partial S^2/\partial v_n$. The commonly known shape $-\partial(sinc^2 v_n)/\partial v_n$ is seen in **Figure 9** in the rear vertical plane, where $\beta = 0$. The constant magnetic field $H_d = \kappa H_0$, where H_0 is the amplitude of the undulator periodic field, produces the bending angle $\theta_H = \frac{2}{\sqrt{3}} \frac{k}{\gamma} \pi N \kappa_1$, resulting in nonzero values of $\beta = \frac{(2\pi nN + v_n)(\gamma\theta_H)^2}{1 + (k^2/2) + (\gamma\theta_H)^2}$ [35, 37, 39] and shifts the maximum of the curve to lower frequencies (see **Figure 9**).
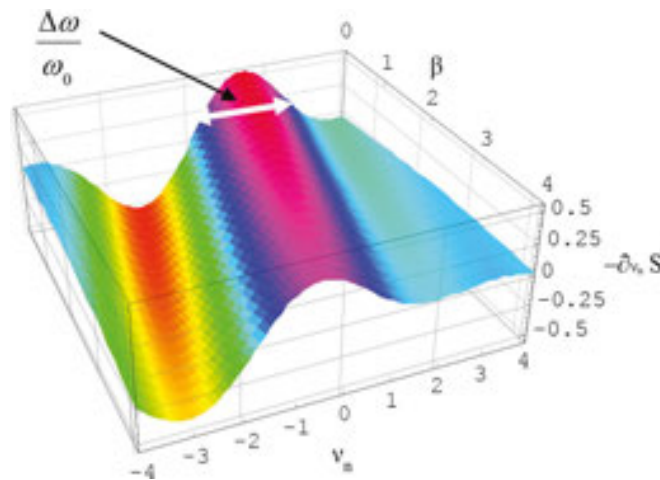

Figure 9. Function $-\dfrac{\partial(S^2(v_n))}{\partial v_n}$, which describes FEL gain in an undulator in external field.

6. High-gain single-pass FELs

There are several reasons why it is more difficult to build free-electron lasers for X-ray region that is for larger wavelengths. First of all, for small wavelengths we need high-energy electrons, but high electron energy also increases the gain length $L_G \propto \gamma$, and we must keep the gain length short, as required for an X-FEL. Then, the undulator parameters H_0 and λ_u must be maximized, keeping in mind, however, that λ_u also determines the radiation wavelength: $\lambda \propto \lambda_u/\gamma^2$. Then, the electron beam current i must be high and its transverse cross section σ small. However, the γ-factor cannot be freely decreased if we want to obtain X-ray wavelengths. These challenges can be better faced in single-pass FELs with typical high-gain regime.

In the high-gain regime the radiation power increases exponentially as the electron beam and radiation co-propagate along the FEL undulator, and this happens on a single pass of the radiation along the FEL. These kinds of FELs are sometime called amplifiers, since everything starts from an initially small source, which may originate as noise, and it can be amplified

by many orders of magnitude before the process saturates. In such FEL, there are no mirrors to form an oscillator cavity and this is particularly good for X-ray region, where mirrors are the most compromised element of the cavity-based FEL. Such FEL essentially works as an amplifier, in which the radiation forms on the single pass through a very long undulator, reaching peak pulse power ~ 10^{10} W for few dozens of femto-seconds. Overwhelming majority of current X-ray FELs are based on this type of design, which has been made possible due to the twenty-first century advances in magnet technology, accelerator constructions, and electron beam production.
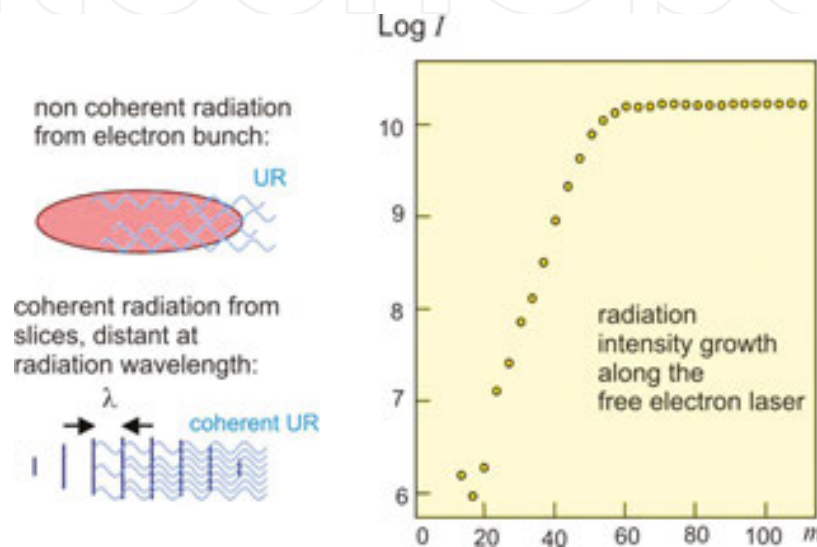

Figure 10. Radiation mechanism in a SASE FEL (amplifier).

The principle of the high-gain FEL interaction is based on the positive feedback process. The electrons emit undulator radiation, which corrects their position in space and their phase with respect to the electromagnetic wave; this groups the electrons on the radiation wavelength scale and thus the more and more coherent radiation is emitted along the undulator. First, the electrons in the bunch have random phases and produce incoherent emission. Already the first waves, emitted by these electrons, trigger formation of microbunches as discussed above (see **Figures 4**, **6** and **10**). Contrary to non-micro-bunched electrons, which emit incoherent waves, the emission of electrons, collected in micro-bunches, which are separated from each other by one wavelength, is correlated (see **Figures 4** and **10**). This causes an exponential intensity increase with the distance that continues until saturation is reached (see **Figure 10**). The schematic drawing in **Figure 10** represents modeling of the performance of the Linac Coherent Light Source—LCLS, with the parameters of the undulator: $L = 100$ m, $\lambda_u = 3$ cm, $L_G = 3.3$ m, $\lambda = 1.5$Å $= 0.15$ nm. The whole installation has the length of $L = 1$ km, current $I = 3$ kA, $E = 13.6$ GeV, Linac and bunch compression: $\gamma\varepsilon_{x,y} = 0.4$ μm (slice), $\sigma_E/E = 0.01\%$ (slice).

Simulation of the electron density in a bunch of the electron beam as it develops from the entrance toward the exit of the undulator is demonstrated in **Figure 11**. Left picture simulates the electron density in the bunch at the beginning of the undulator, middle picture

represents the simulation in the middle of the undulator length, and the right picture demonstrates the electron density in the bunch at the end of the undulator.
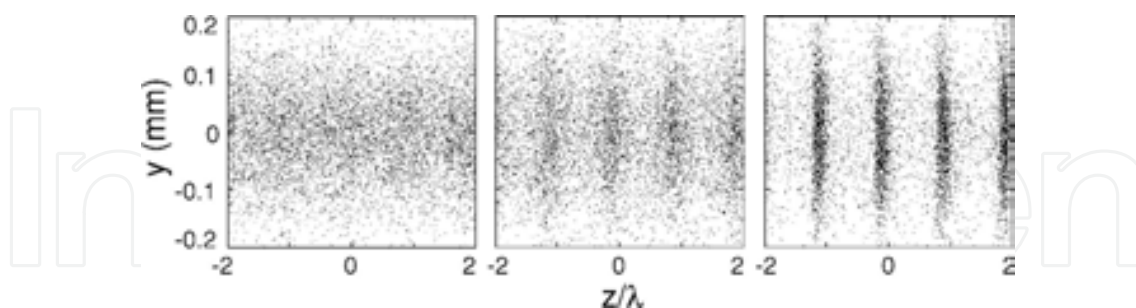

Figure 11. Simulation of the density modulation of the electron beam along the undulator: undulator beginning—left picture, undulator middle—middle picture, undulator end—right picture.

The transverse structure of the electron bunch is much larger than its longitudinal substructure. Note the length between the slices can be of the order of nm, and there can be up to hundreds of thousands of slices in a bunch.

7. Some advanced single-pass FEL schemes

Perhaps, the most common development of the basic SASE FEL scheme, where the amplification starts from noise with random phase, is represented by SASE FEL with seeding. In this case, already at the beginning of the undulator, unbunched electrons with random phase interact with coherent laser seed radiation, which bunches them accordingly. This scheme has the advantage of the stability of the phase, because the process is controlled by the seeding laser.
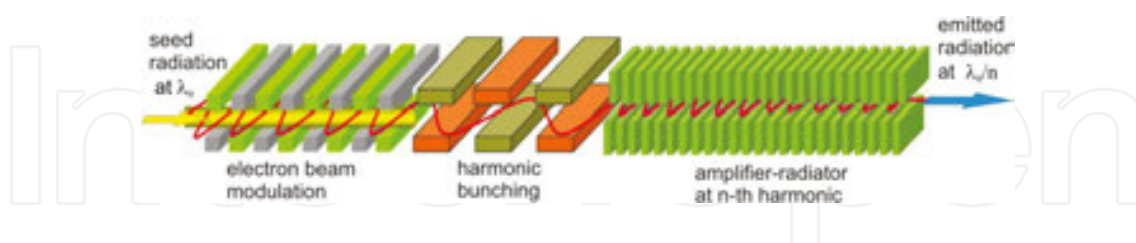

Figure 12. HGHG FEL with laser seed, harmonic generator, buncher, and amplifier.

To achieve extremely high frequencies, for example, those of the X-ray band, the following modification of SASE FEL with high-gain harmonic generation (HGHG) is sometimes employed (see schematic drawing in **Figure 12**).

It consists of the seed laser, harmonic generator, and the amplifier. The coherent seed laser radiation first passes the short undulator, called modulator, which is tuned to the seed frequency. The interaction with the electron beam gives the latter small longitudinal energy modulation. The following section of the installation converts this energy modulation into a

beam density modulation in a magnetic dispersion unit. Then the modulated electron beam and the UR pass the second undulator, which is tuned to the nth harmonic of the modulator. When they pass the second undulator, the nth harmonic of the UR is fully amplified to saturation levels in this second undulator, frequently called radiator. At the exit the pulses with <20 fs duration can be obtained.

One of the most important advantages of the mirror FEL is the possibility to select optical modes with the help of the mirrors. SASE FEL in its classical scheme is lacking this ability: there are no mirrors, which, in turn, gives other advantages. Together the advantage of the cavity-based mirror design with those of SASE FEL, the magnetic chicanes (small blocks in **Figure 13**) can be introduced between a sequence of undulators (big blocks in **Figure 13**) to impose a sort of mode locking in mirrorless single-pass FEL. The proper scheme is given in **Figure 13**.
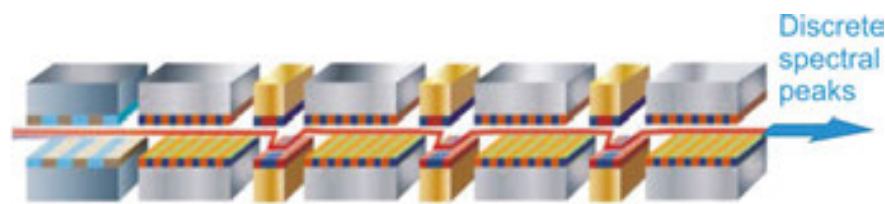

Figure 13. SASE FEL design with chicane mode-locking (big blocks are undulators, small blocks are chicanes).
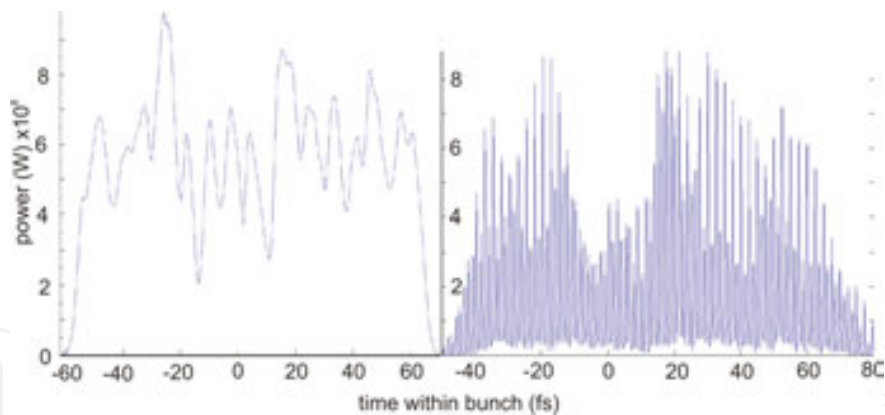

Figure 14. SASE output power after the undulator without (left) and with (right) chicanes.

The magnetic chicanes introduce an extra slippage of the radiation with respect to the electron bunch. Only those radiation wavelengths that have an integer number fit into the relative slippage of the radiation with respect to the electron bunch in one module will remain phase-matched. Only they will constructively interfere over many such modules. In this way form the modes of the radiation field, which create a comb of equally spaced modes in the output frequency spectrum. Such a mode locking can be achieved by the beam energy modulation or by a beam current modulation of the same period. The result is similar to that created by the optical mode locking. We present the example of the power output and the spectrum of a

common SASE FEL (see **Figures 14** and **15** left, respectively) to compare it with the example of the power output and of the spectrum of a FEL with chicane mode locking (see **Figures 14** and **15** right, respectively). Note that instead of the relatively broad SASE FEL spectrum, we now see the series of sharp equidistant peaks. The same regards the output power. At the end of the undulator-chicane line we achieve higher spectral power from the FEL.
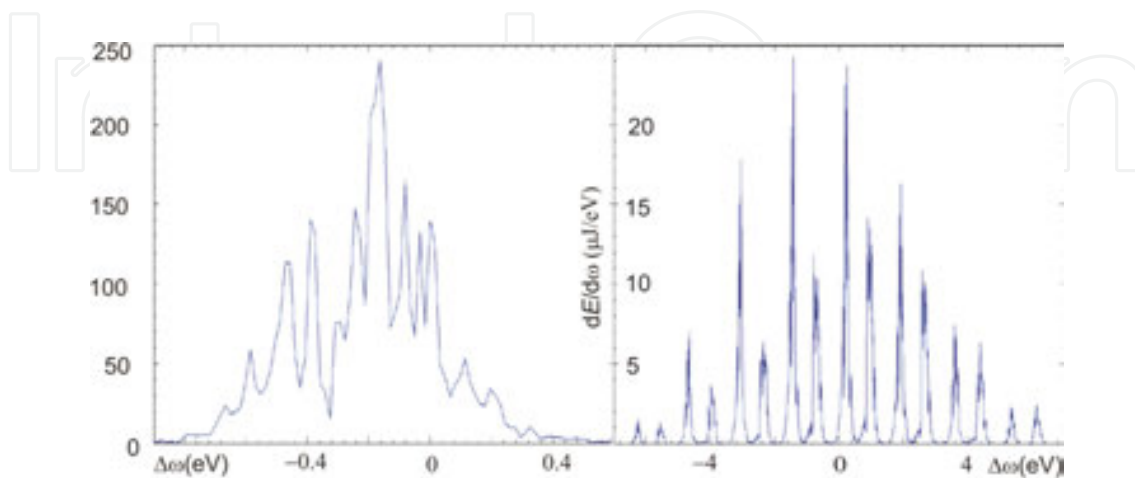

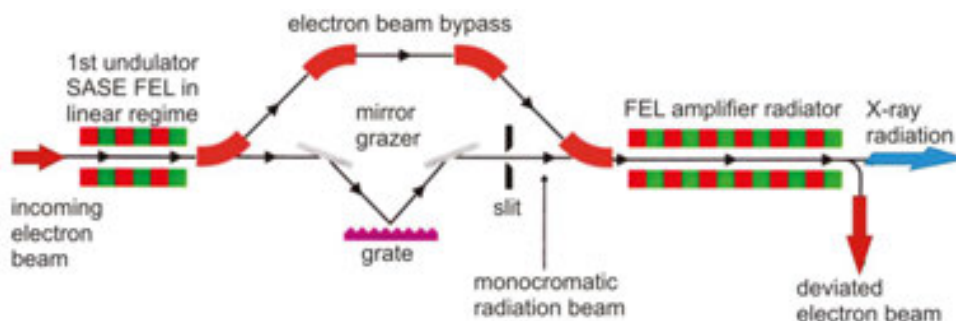**Figure 15.** SASE spectrum after the undulator without (left) and with (right) chicanes.

Figure 16. Schematic design of a self seed FEL.

Eventually, we touch on the functioning of the so-called self-seed FEL scheme, demonstrated in **Figure 16**. The advantage of this type of FELs consists in that they are independent of any external radiation source, which must be otherwise very stable and precisely matched to the electron beam in space and time. Both undulators in the self-seed design are tuned to the same frequency. First undulator is in essence a short SASE FEL, which operates in the linear gain regime far from the saturation level. It produces the radiation in the form of typical SASE FEL pulses at the power level approximately 1000 times below the saturation level. Then the electron beam is fed through a magnetic chicane, which eliminates the density modulation, introduced in the first undulator, and delays the electron bunch to match the UR pulse at the next undulator. The radiation from the first undulator, which works in linear regime, is spectrally filtered by a narrow-band grating monochromator. The latter stretches the radiation pulse, where the coherence length now exceeds that of the electron bunch. After all, the

reshaped radiation pulse and the delayed electron bunch meet. The filtered UR becomes the seed for the second undulator—radiator—which amplifies the UR to saturation level.
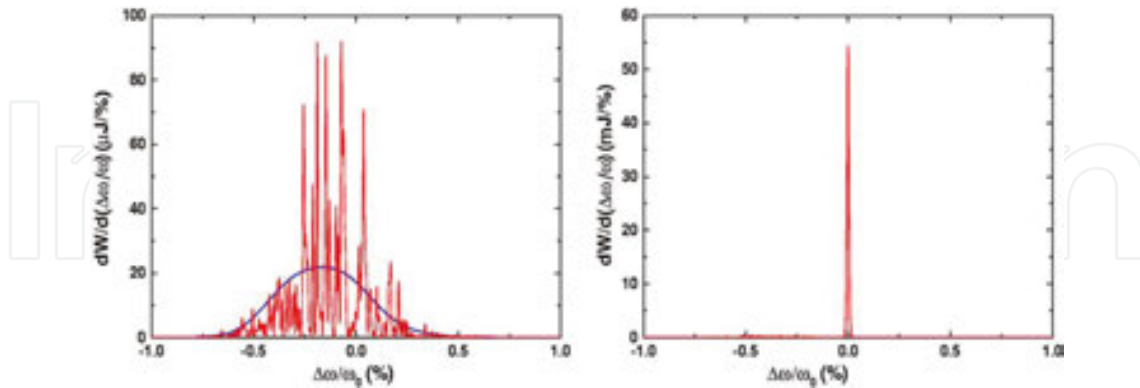

Figure 17. Spectrum after the first SASE FEL and after the second undulator-amplifier.

Not only this FEL is independent on any external radiation source, but due to its design it also produces remarkably good radiation pulses with given characteristics.

In **Figure 17** we demonstrate the example of the output characteristics of such a self-seed FEL. Note that the spectral power distribution after the first (left) and the second undulator (right) differ from each other. The common SASE FEL spectrum (left) is rather broad and consists of many spectral lines even far below the saturation level. The output radiation on the contrary represents a narrow spectral line with only a small background of spontaneous radiation (right). Spectral brightness has increased by almost two orders of magnitude.

8. Challenges and future developments of X-ray FELs

To conclude the review of some of the most prominent for X-FEL schemes, let us formulate main challenges for the X-ray FEL:

1. The radiation wavelength $\lambda = \frac{\lambda_u}{2\gamma^2}\left(1 + \frac{k^2}{2}\right)$ should be reduced to 1 Å. For small wavelengths we need high-energy electrons, but high electron energy also increases the gain length L_G. Longer undulator period λ_u also determines longer radiation wavelength λ and longer gain length L_G.

2. The electron beam energy has to be 10–20 GeV. There is a compromise to contain the gain length and obtain short wave radiation.

3. The gain length $L_G = \frac{1}{\sqrt{3}}\left(\frac{4mc}{\mu e}\frac{\gamma^3\lambda_u}{k^2}\frac{\sigma_r^2}{I}\right)^{1/3}$ has to be contained preferably about of 10 m or so.

   Note that $\frac{\sigma_r^2}{I} = \frac{\sigma_r^2 L_{bunch}}{qc}$, where L_{bunch} is the longitudinal size of the bunch and q is the electric charge.

4. The electron beam current I must be high and its transverse cross section σ small. However, the γ-factor cannot be freely decreased if we want to obtain X-ray wavelengths.

5. As follows from the expression for L_G high peak current is requested for it, such as $I \sim \text{kA}$ or more.

6. Transverse electron beam size has to be small, possibly $\sigma_R \sim 10$ μm or so.

7. The energy spread of the electron beam σ_e has to be as small as possible, preferably $\sigma_e \approx 10^{-4}$ or less.

8. The electron and the photon beams have to be overlapped properly.

Note also that in the light of the above said the following requirements arise for the electron beam in transverse: low emittance of the beam and preservation of this low emittance; for the longitudinal dimension good compression and acceleration are required. The main negative factors, which affect the amplification, are the electron energy spread, the angular divergence, the transverse electron beam size, the diffraction of the wave and others. The electron energy spread has negative effect on both the amplification and FEL saturation level. Amplification mainly starts with the optimal electron energy, whose γ-factor determines the wavelength. As the energy is transferred from the electrons to the radiated electromagnetic wave, the energy of the electrons naturally decreases. The wave emissions from all the electrons differ from each other, because different electrons have different energies. After the wave-electron interaction, the electron beam energy spread increases and at a certain point it grows to a level, where no gain occurs. Moreover, well before the electrons loose a substantial portion of their energy, they slow down by emitting electro-magnetic energy and change their phase with respect to the wave. Thus they begin to take the energy from the wave rather than giving it.

In conclusion, let us state some areas, where the performance of the X-ray sources of coherent radiation can be further improved. First of all, the temporal coherence of SASE FELs can be improved. The improved temporal coherence would in turn improve the spectral brightness of the sources, which means the users will have more useful photons. The way to accomplish it could consist, for example, in seeding X-FEL from a radiation source with good temporal coherence.

An alternative approach to single-pass high-gain amplifier schemes is to use cavity feedback in a relatively low-gain system. The development of relatively high-reflectivity diamond crystal mirrors in the X-ray regime makes them feasible.

Reducing X-ray pulse durations to the attosecond regime will provide spatiotemporal resolution of atomic processes. Two techniques have so far been reported that can take pulse durations significantly below 100 as toward the atomic unit of time 24 as. The first technique employs a variation of an echo-enabled harmonic generation method and produces pulses of ~20 as duration at a wavelength of 1 nm with the power, which in peaks reaches ~200 MW. The second technique is based on mode-locking in conventional cavity lasers—oscillators. It could generate radiation at 1.5 Å wavelength in sequences of pulses with ~150 as intervals

between them. The peak power in each pulse could reach ~5 GW and the duration of the pulse could be as short as ~20 as.

Eventually, γ-ray FEL would be extremely interesting for studying nuclear processes. This may be the future of X-FEL.

Author details

K. Zhukovsky

Address all correspondence to: zhukovsk@physics.msu.ru

Department of Theoretical Physics, Physical Faculty, M.V. Lomonosov Moscow State University, Leninskie Gory, Moscow

References

[1] Ginzburg VL. "On the radiation of microradiowaves and their absorbtion in the air". *Isvestia Akademii Nauk SSSR (Fizika)*, vol. 11, N 2, 947, 1651.

[2] Motz H, Thon W, Whitehurst RNJ. "Experiments on radiation by fast electron beams". *Appl. Phys.*, vol. 24, 826, 1953.

[3] Artcimovich AL, Pomeranchuk IJ. "Radiation from fast electrons in a magnetic field". *J. Phys. USSR*, vol. 9, 267, 1945.

[4] Ternov IM, Mikhailin VV, Khalilov VR. *Synchrotron Radiation and its Applications*, Harwood Academic Publishers, Chur, London, Paris, New York, 1985.

[5] Alferov DF, Bashmakov YuA, Bessonov EG. "Radiation of relativistic particles in an undulator". *Sov. Phys. Tech. Phys.*, vol. 17, N 9, 1540, 1973.

[6] Alferov DF, Bashmakov UA, Cherenkov PA. "Radiation from relativistic electrons in a magnetic undulator". *Uspehi Fisicheskih Nauk*, vol. 32, 200, 1989.

[7] Bordovitsyn VA (Ed.), *Synchrotron Radiation Theory and its Development: in the Memory of I.M.Ternov*. Series on Synchrotron Radiation Technique and Applications, vol. 5, World Scientific Publishing, Singapore, 1999.

[8] Bessonov EG, Gorbunkov MV, Ishkhanov BS, Kostryukov PV, Maslova Yu YA, Shvedunov VI, Tunkin VG, Vinogradov AV. Laser-electron generator for X-ray applications in science and technology, *Laser Part. Beams*, vol. 26, N 3, 489–495, 2008.

[9] Mcneil BWJ, Thompson NR. X-ray free-electron lasers, *Nat. Photon.*, vol. 4, N 12, 814–821, 2010. doi: 10.1038/nphoton.2010.239.

[10] Sokolov AA, Ternov IM. *Radiation from Relativistic Electrons* (edited by C.W. Kilmister), American Inst. of Physics, New York, 1986.

[11] Feldhaus J, Sonntag B. Strong field laser physics. *Springer Ser. Opt. Sci.*, vol. 134, 91, 2009.

[12] Zholents AA. "Attosecond X-ray pulses from free-electron lasers". *Laser Phys.*, vol. 15, N 6, 855, 2005.

[13] Bessonov EG. Light sources based on relativistic electron and ion beams. *Proc. SPIE*, vol. 6634, 66340X, 2007.

[14] Zhukovsky KV. "Harmonic radiation in a double frequency undulator with account for broadening". *Moscow Univ. Phys. Bull.*, vol. 70, N 4, 232, 2015.

[15] Zhukovsky K. "Undulator radiation in multiple magnetic fields". *Synchrotron: Design, Properties and Applications*, vol. 39, Nova Science Publishers Inc., USA, 2012.

[16] Zhukovsky K. "Harmonic Generation by ultrarelativistic electrons in a planar undulator and the emission-line broadening". *J. Electromagn. Wave*, vol. 29, N 1, 132–142, 2015.

[17] Tripathi S, Mishra G. "Three frequency undulator radiation and free electron laser gain". *Rom. J. Phys.*, vol. 56, N 3–4, 411, 2011.

[18] Mishra G, Gehlot M, Hussain J-K. "Spectral properties of bi-harmonic undulator radiation". *Nucl. Instrum. A*, vol. 603, 495, 2009.

[19] Dattoli G, Mikhailin VV, Ottaviani PL and Zhukovsky K. "Two-frequency undulator and harmonic generation by an ultrarelativistic electron". *J. Appl. Phys.*, vol. 100, 084507, 2006.

[20] D. Iracane and P. Bamas, "Two-frequency wiggler for better control of free-electron-laser dynamics", Phys. Rev. Lett. 67 (1991) 3086.

[21] V. N. Korchuganov, N. U. Sveshikov, N. V. Smolyakov, C. I. Tomin, "Special-purpose radiation sources based on the Siberia-2 storage ring", *J. Surf. Invest.: X-ray, Synchrotron and Neutron Tech.*, Vol.11, p. 22, 2010.

[22] Walker RP. "Interference effects in undulator and wiggler radiation sources". *Nucl. Instrum. Methods*, vol. A335, 328, 1993.

[23] Onuki H, Elleaume P. *Undulators, Wigglers and Their Applications*, Taylor & Francis, New York, 2003.

[24] Vagin PV, Englisch U, Müller T, et al.. "Commissioning experience with insertion devices at PETRA III". *J. Surf. Invest.: X-ray, Synchrotron Neutron Tech.*, vol. 6, N 5, 1055, 2011.

[25] Hussain J, Gupta V, Mishra G. "Effect of two-peak beam energy spread on harmonic undulator radiation and free-electron laser gain". *Nucl. Instrum. A*, vol. 608, 344, 2009.

[26] Reiss HR. "Effect of an intense electromagnetic field on a weekly bound system". *Phys. Rev.*, vol. A22, 1786, 1980.

[27] Smolyakov NV. "Focusing properties of a plane wiggler magnetic field". *Nucl. Instrum. A*, vol. 308, 83–85, 1991.

[28] Hussain J, Mishra G. "Harmonic undulator radiations with constant magnetic field". *Opt. Commun.*, vol. 335, 126, 2015.

[29] Dattoli G, Mikhailin VV, Zhukovsky KV. "Influence of a constant magnetic field on the radiation of a planar undulator". *Moscow Univ. Phys. Bull.*, vol 64, 507, 2009, c/c of Vestnik Moskovskogo Universiteta Ser. 3 Fizika Astronomiya, vol. 5, 33, 2009.

[30] Mikhailin VV, Zhukovsky KV, Kudiukova AI. "On the radiation of a planar undulator with constant magnetic field on its axis taken into account". *J. Surf. Invest.: X-ray Synchrotron Neutron Tech.*, vol. 8, N 3, 422, 2014.

[31] Dattoli G, Mikhailin VV, Zhukovsky K. "Undulator radiation in a periodic magnetic field with a constant component. "*J, Appl. Phys.*, vol. 104, 124507, 2008.

[32] K. Zhukovsky, "Emission and tuning of harmonics in a planar two-frequency undulator with account for broadening", *Laser Part. Beams*, 2016, doi: 10.1017/S0263034616000264

[33] Mirian NS, Dattoli G, DiPalma E, Petrillo V. "Production and properties of two-color radiation generated by using a Free-Electron Laser with two orthogonal undulators". *Nucl. Instrum. A*, vol. 767, 227, 2014.

[34] Zhukovsky K. "Inhomogeneous and homogeneous losses and magnetic field effect in planar undulator radiation". *Prog. Electromagn. Res. B*, vol. 59, 245, 2014.

[35] Zhukovsky K. "Analytical account for a planar undulator performance in a constant magnetic field". *J. Electromagn. Wave*, vol. 28, N 15, 1869, 2014.

[36] Zhukovsky KV. "A model for analytical description of magnetic field effects and losses in a planar undulator radiation". *J. Surf. Invest.: X-ray Synchrotron Neutron Tech.*, vol. 8, N 5, 1068, 2014.

[37] Zhukovsky K., High harmonic generation in undulators for FEL, *Nuclear Instrum. Methods Phys. Res. B*, vol. 369, 9–14, 2016, DOI: 10.1016/j.nimb.2015.10.041.

[38] Quattromini M, Artioli M, Di Palma E, Petralia A, Giannessi L. Focusing properties of linear undulators, *Phys. Rev. ST Accel. Beams*, vol. 15, 080704, 2012, DOI: 10.1103/PhysRevSTAB.15.080704.

[39] Zhukovsky K. "High harmonic generation in the undulators for free electron lasers". *Opt. Commum.*, 353, 35–41, 2015.

[40] Dattoli G, Srivastava HM, Zhukovsky K. "Orthogonality properties of the Hermite and related polynomials". *J. Comput. Appl. Math.*, vol. 182, 165–172, 2005.

[41] Dattoli G, Srivastava HM, Zhukovsky K. "A new family of integral transforms and their applications". *Integral Transform. Spec. Funct.*, vol. 17, N 1, 31–37, 2006.

[42] Dattoli G, Zhukovsky K. "Evolution of time dependant linear potentials and non-spreading airy wave packets". *Appl. Math. Comput.*, V 217, 7966–7974, 2011.

[43] Zhukovsky KV. "A method of inverse differential operators using ortogonal polyno-mials and special functions for solving some types of differential equations and physical problems". *Moscow Univ. Phys. Bull.*, vol. 70, N 2, 93–100, 2015, DOI: 10.3103/S0027134915020137 .

[44] Zhukovsky K. "Solution of some types of differential equations: operational calculus and inverse differential operators". *Sci. World J.*, vol. 2014, 8 pages, 2014, article ID 454865.

[45] Zhukovsky KV. "Operational method of solution of linear non-integer ordinary and partial differential equations". *SpringerPlus*, vol. 5, 119, 2016, DOI: 10.1186/s40064-016-1734-3.

[46] Jackson JD, *Classical Electrodynamics*. 2nd ed., Wiley, New York, 1975.

[47] Madey JMJ. Stimulated emission of bremsstrahlung in a periodic magnetic field. *J. Appl. Phys.*, vol. 42, 1906–1913, 1971.

[48] Margaritondo G, Rebernik Ribic P. A simplified description of X-ray free-electron lasers. *J. Synchrotron Rad.*, vol. 18, 101–108, 2011.